Real-time Evaluation of Ant Lion Optimizer tuned Linear Matrix Inequalities based State Feedback Controller for the Control of an Under-actuated System

P. Komakhan Sudar Vendan[*#], J. Kanakaraj[*], S. Rajan[**]

[*] *Electrical and Electronics Engineering Department, PSG College of Technology, Coimbatore, India*
[#]*(Tel: +91 96006 75612; e-mail: ksv.eee@psgtech.ac.in).*
[**]*Instrumentation and Control Systems Engineering Department, PSG College of Technology, Coimbatore, India*

Abstract: The stabilization and trajectory tracking control problem of the classical benchmark Under-actuated cart-inverted pendulum system is addressed. In the Linear Matrix Inequality (LMI) based State Feedback Controller (SFC), the LMI regions are selected by cumbersome trial and error methods where optimal results are not always guaranteed. Hence in this work, the optimization algorithms are proposed to tune the LMI region in the LMI based SFC. The Ant Lion Optimizer (ALO) is proposed to tune the LMI regions of the SFC for the control problem. The ALO algorithm finds the optimal LMI region from the solution of the inequality problem, which results in the optimal state feedback gain, minimising trajectory tracking error while stabilising the pendulum in the unstable upright position. The performance of the proposed ALO tuned LMI based SFC is presented and compared with the LMI based SFC without optimization and APSO tuned LMI based SFC scheme. The suggested controller's real-time viability is demonstrated by incorporating it in Quanser's IP02 benchmark Cart-inverted pendulum system and the results show a 41.97 percentage reduction in Integral Square Error (ISE) of trajectory tracking with improved transient response while stabilizing the pendulum in the unstable position when compared to the controllers in comparison.

Keywords: Ant Lion Optimizer; Inverted Pendulum; Linear Matrix Inequality; Stabilization; tracking; experiment design; real-time evaluation.

1. INTRODUCTION

The cart inverted pendulum is a benchmark under-actuated control problem studied to design new controllers. This system is nonlinear, inherently unstable and a controller is needed to provide a stable operation. To evaluate the effectiveness of the suggested controllers, the newly built or modified control algorithms are evaluated in benchmark systems. Many real-time control challenges, such as Segway, the human posture systems, Pendubots, the launching of a rocket and earthquake-resistant buildings, can benefit from the intended controllers for such a complex process. This benchmark system poses two control problems (Shahab et al., 2017). The first control problem is to swing up the pendulum from its initial rest position and the second control problem is to stabilize the pendulum in the upright position which is highly unstable in nature. The stabilization problem of the cart-inverted pendulum has resulted in a variety of advanced control algorithms. The stabilization of the pendulum started with a simple State Feedback Controller (SFC) which then incorporated the PI controller via State-PI Feedback (Wiboonjaroen and Sujitjorn, 2011). Several controllers (Blondin and Pardalos, 2020; Roose et al., 2017; Irfan et al., 2018; de Jesús Rubio, 2018; Franco et al., 2018) are designed to control the pendulum. The controllers are focused on optimizing the control effort needed for stabilizing the pendulum. The Linear Quadratic Regulator (LQR) based SFC is an optimal control method for the stabilization problem which achieves robust stabilization of the inverted pendulum even in the presence of disturbance (Vinodh Kumar and Jerome, 2013). In this method, the Algebraic Riccati Equation (ARE) is solved to get the closed-loop feedback gain of the system. Here, the selection of weighting matrices affects the solution of the ARE, which in turn affects the closed-loop performance of the system. Since there are no standard procedures to select the weighting matrices of the LQR, the performance of the method hinges on the random initial selection of weights. The solution of the ARE in LQR is then addressed by heuristic soft computing methods that optimize the control problem. The Genetic Algorithm tuned LQR (Li et al., 2007), Particle Swarm Optimization (PSO) tuned LQR (Chang et al., 2012), (Assahubulkahfi et al., 2018) and Adaptive Particle Swarm Optimization (APSO) tuned LQR (Kumar E. and Jerome, 2014), (Vinodh Kumar et al., 2016) are few state feedback control schemes that use soft computing techniques to find the optimal state feedback gain.

The complex convex optimization development resulted in the feasibility of the solution for LMIs by the computer for which finding the manual solution is extremely difficult and time-consuming (Boyd et al., 1994). (Scherer et al., 1997) proposed an LMI optimization-based multiobjective output feedback control. Then, a simple state feedback controller using pole region constraint was proposed by (Werner et al., 2003) for power system stabilizers. For time-delay systems, observer-based controller design by LMI optimization was proposed by (Kwon et al., 2006). Robust control design via LMI optimization was proposed by (Adegas and Stoustrup, 2011). Robust stabilization of underactuated systems by Lyapunov redesign was proposed by (Ravichandran and Mahindrakar, 2011). Grid connected converters under uncertain conditions are controlled by LMI based optimized control (MacCari et al., 2014). The feedback gain of the LMI based SFC proposed by (Garone and Ntogramatzidis, 2015) in the globally monotonic control algorithm is found by solving a set of inequality equations which included the stability conditions and proper selection of LMI region. (Ntogramatzidis et al., 2016) proposed the globally monotonic LMI based SFC for MIMO systems. (Muhammad, 2018) proposed LMI based SFC with the constraints of closed-loop poles in the desired LMI region addressed by pole placement for the under-actuated gantry crane system. The location of poles in the LMI region guarantees stable operation but to find the one that gives minimum tracking error by arbitrary pole placement is difficult and time-consuming. Optimal performance is not always guaranteed by this method. Robust SFC based on LMIs for grid-connected converters is proposed by (Koch et al., 2019). Optimized Proportional-Derivative sliding mode control based on LMIs are proposed by (Ghaffari, 2020). Instead of the conventional change of variables method in LMI formulation, the state feedback gains are taken as optimization variables by (Felipe and Oliveira, 2021). High processing speed processors developed in recent years enabled the research in several optimization problems. Thus, from the literatures it is seen that the optimization is concentrated on different LMI parameters except the variables defining the LMI region. Also, it is observed that pole placement and LMI region selection is done by arbitrary trial and error methods. Hence, the optimization algorithms are proposed to be used to tune the LMI region in the proposed work.

In the proposed work, a simple LMI based SFC is first designed using the basic Lyapunov method and the inequalities proposed by (Garone and Ntogramatzidis, 2015). The conditions are then added in the inequality problem such that the proper LMI region as stated by (Werner et al., 2003) is added to get the optimal response. This selection of LMI region by trial and error method is cumbersome and hence optimization algorithms are proposed to find the LMI region which gives the optimal performance of the SFC. Several optimization techniques inspired by nature have been created. Firefly algorithm (Yang and He, 2013), Ant Lion Optimizer (Mirjalili, 2015; Abualigah et al., 2008; Zhang et al., 2019), Whale Optimization (Mirjalili and Lewis, 2016), Grasshopper optimization algorithm (Saremi et al., 2017), Cuckoo Search algorithm (Yang and Deb, 2014), Grey Wolf Optimizer (Mirjalili et al., 2014), Salp Swarm Optimizer (Mirjalili et al., 2017), Flower Pollination (Alyasseri et al., 2018), Bat Algorithm (Huang and Ma, 2020), African Vultures Optimizer (Abdollahzadeh et al., 2021) are few of the recently developed algorithms. In the proposed work, Ant Lion Optimizer is used to tune the LMI based SFC to select proper LMI region which in turn gives the optimal state feedback gains for the control problem. Unlike PSO and its variants, the ALO does not require any pre-requisite information relating to the parameter initialisation. The parameters such as inertial weights and velocity in the PSO method need to be properly chosen else there are more chances for the optimization to get trapped with the local optimum. Since the ALO method does not have such constraints, it results in a better global optimum value within the search space. The proposed ALO tuned LMI based SFC is compared with the LMI based SFC without optimization (Garone and Ntogramatzidis, 2015) and APSO tuned LMI based SFC. The results are then validated with real-time implementation. In the current work, the stabilization problem of the inverted pendulum is considered. Simulation results are taken for the common operating conditions with a square wave trajectory for the cart to track while stabilizing the pendulum. The Integral Square Error (ISE) is taken as the performance index for analysing the controller's performance. With the justification of the simulation results along with the performance index, the experimental setup is made. The real-time evaluation result also justifies the ALO tuned LMI based SFC's performance. The following is a breakdown of the paper's structure: Section 1 gives a brief introduction to the control problem considered along with the recent developments. Section 2 deals with the system description. Section 3 focuses on the modeling of the Cart-Inverted Pendulum system. Section 4 deals with the controller design. Section 5 covers the results with the discussions. Section 6 concludes with the observations from the results.

2. CART - INVERTED PENDULUM SYSTEM

The moving cart-inverted pendulum systems (CIPS) schematic representation is shown in Figure 1. The under-actuated cart-inverted pendulum nonlinear system has two degrees of motion. The system has a single control input voltage given to the motor and has 2-Degrees of Freedom (DOF) outputs and such systems are difficult to control. The first output is the linear motion of the cart in the railings provided by the gear arrangements. The second output is the angular motion of the pendulum. Because of this nature, this setup is used for designing controllers for Single Input Multiple Output (SIMO) Systems. The inverted pendulum framework comprises of a mass M_p pendulum with a length l_p coupled to a mass M_c of the cart. The cart has a motor attached to it. The control input voltage given to the motor drives the cart along the railing through gear arrangements. The cart's mass M_c is inclusive of an additional weight M_w which is attached to the cart for balancing the pendulum's weight. The cart can only move in one direction: horizontally, whereas the pendulum freely revolves in the x-y plane.

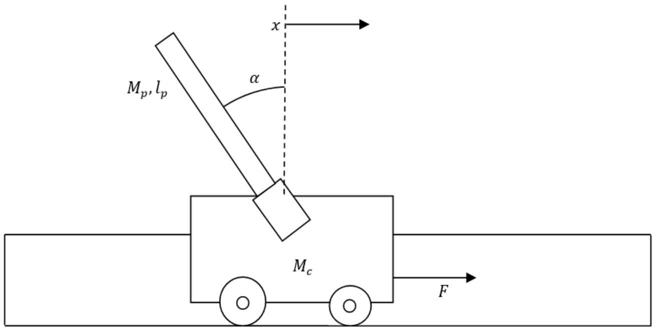

Fig. 1. Setup of Cart-Inverted Pendulum.

As a result, the state variables are taken as the cart displacement 'x_c' in the horizontal direction and the pendulum angle 'α'.

3. MATHEMATICAL MODELLING OF INVERTED PENDULUM SYSTEM

The energy equations of the Euler-Lagrangian method are used to obtain the inverted pendulum's mathematical model. The energy terms are differentiated with respect to the state variables in the Lagrangian formulation. This method is simpler to use when the system becomes complex. Two generalized equations governing the Lagrangian method are as follows: one for the linear motions whereas the other is for the rotational motions. The effectiveness of this method makes it ideal for use in the modeling of the inverted pendulum setup which has the cart's translational motion as well as the pendulum's rotational motion. (Quanser Inc., 2007)

3.1 Euler – Lagrangian Formulation

The general form of the Lagrangian Ln is given by Eqn. 1.

$$Ln = KE - PE \tag{1}$$

Where KE and PE corresponds to that of the total kinetic energy and potential energy of the system respectively.

$$KE = \frac{1}{2}\left(M_c + M_p\right)\dot{x}_c{}^2\,(t) - M_p l_p \cos\big(\alpha(t)\big)\,\dot{\alpha}(t)\dot{x}_c(t)$$

$$+\tfrac{1}{2}\left(I_p + M_p l_p{}^2\right)\dot{\alpha}^2\,(t) \tag{2}$$

For the inverted pendulum setup, the linear translational motion is given by the cart's position x_c and the rotational motion is given by pendulum position α. The total Kinetic Energy of the system is given by Eqn. 2 and the total Potential Energy of the system is given as in Eqn. 3.

$$PE = M_p g l_p \cos\big(\alpha(t)\big) \tag{3}$$

The Euler-Lagrangian for the inverted pendulum system is given by Eqn. 4.

$$F_i = \frac{d}{dt}\frac{\partial Ln}{\partial \dot{x}_c} - \frac{\partial Ln}{\partial x_c} \tag{4}$$

$$T_i = \frac{d}{dt}\frac{\partial Ln}{\partial \dot{\alpha}} - \frac{\partial Ln}{\partial \alpha} \tag{5}$$

Where F_i is the translational force and T_i is the rotational force exerted on the x_c and α co-ordinates respectively. The forces are given by the below expressions.

$$F_i = F_c(t) - B_{eq}\dot{x}_c \text{ and } T_i = -B_p\dot{\alpha}(t) \tag{6}$$

The nonlinear model obtained by the Euler-Lagrangian method is given by Equations (7) and (8).

$$\begin{aligned}\left(M_c + M_p\right)\ddot{x}_c\,(t) &= F_c(t) - B_{eq}\dot{x}_c(t)\\ &+ M_p l_p \cos\big(\alpha(t)\big)\,\ddot{\alpha}(t) - M_p l_p \sin\big(\alpha(t)\big)\,\dot{\alpha}^2(t)\end{aligned} \tag{7}$$

$$\left(I_p + M_p l_p{}^2\right)\ddot{\alpha}\,(t) = M_p l_p \cos\big(\alpha(t)\big)\,\ddot{x}_c(t) - B_p\dot{\alpha}(t) + M_p g l_p \sin\big(\alpha(t)\big) \tag{8}$$

The nonlinear model represented by Eqn. 7 and 8 can be linearized around the equilibrium point (upright pendulum position) such that $sin(\alpha) \cong \alpha, cos(\alpha) \cong 1$, and the higher-order terms in the models are also neglected for simplicity. The linearized approximated model is represented in state-space to design the state feedback controller for upright pendulum stabilization.

$$\dot{X} = AX + BU \tag{9}$$

$$Y = CX \tag{10}$$

Where, $X = [x_c\ \alpha\ \dot{x}_c\ \dot{\alpha}]^T, U = V\ and\ Y = [x_c\ \alpha\ \dot{x}_c\ \dot{\alpha}]^T$. The inverted pendulum setup's state-space model is depicted in Eqn. 11.

$$A = \begin{bmatrix} 0 & 0 & 1 & 0\\ 0 & 0 & 0 & 1\\ 0 & \frac{gM_p^2 l_p^2}{(M_p+M_c)I_p+M_cM_pl_p^2} & \frac{-B_{eq}(M_pl_p^2)}{(M_p+M_c)I_p+M_cM_pl_p^2} & \frac{-M_pl_pB_p}{(M_p+M_c)I_p+M_cM_pl_p^2}\\ 0 & \frac{M_pgl_p(M_p+M_c)}{(M_p+M_c)I_p+M_cM_pl_p^2} & \frac{-M_pl_pB_{eq}}{(M_p+M_c)I_p+M_cM_pl_p^2} & \frac{-(M_p+M_c)B_p}{(M_p+M_c)I_p+M_cM_pl_p^2}\end{bmatrix}$$

$$B = \begin{bmatrix} 0\\ 0\\ \frac{I_p+M_pl_p^2}{(M_p+M_c)I_p+M_cM_pl_p^2}\\ \frac{M_pl_p}{(M_p+M_c)I_p+M_cM_pl_p^2}\end{bmatrix} \quad C = \begin{bmatrix}1&0&0&0\\0&1&0&0\\0&0&1&0\\0&0&0&1\end{bmatrix} \tag{11}$$

The values of the parameters of the inverted pendulum setup listed in Table 1 are substituted in Eqn. 11 to get the state-space model (Quanser Inc., 2007).

Table 1. The inverted pendulum's system parameters.

Parameter	Description	Value
M_c	cart mass	1.0731 Kg
M_p	Pendulum mass	0.127 Kg
l_p	Length of the Pendulum	0.1778 m
I_p	Pendulum moment of Inertia	1.2 $\times 10^{-3}\ Kgm^2$
g	Acceleration due to gravity	9.81 m/s^2
B_p	Viscous damping co-efficient at Pendulum axis	0.0024 Nms/rad
B_{eq}	Viscous damping co-efficient at the motor pinion	5.4 Nms/rad

The parameters are substituted in Eqn. 11 and the inverted pendulum setup's state-space model obtained is shown by Eqn. (12) and (13).

$$\begin{bmatrix}\dot{x}_c\\ \dot{\alpha}\\ \ddot{x}_c\\ \ddot{\alpha}\end{bmatrix} = \begin{bmatrix}0 & 0 & 1 & 0\\ 0 & 0 & 0 & 1\\ 0 & 1.3101 & -5.8717 & -0.0142\\ 0 & 48.1625 & -25.4309 & -0.5218\end{bmatrix}\begin{bmatrix}x_c\\ \alpha\\ \dot{x}_c\\ \dot{\alpha}\end{bmatrix} + \begin{bmatrix}0\\ 0\\ 1.3655\\ 5.9142\end{bmatrix}u \tag{12}$$

$$Y = \begin{bmatrix}1&0&0&0\\0&1&0&0\\0&0&1&0\\0&0&0&1\end{bmatrix}\begin{bmatrix}x_c\\ \alpha\\ \dot{x}_c\\ \dot{\alpha}\end{bmatrix} \tag{13}$$

4. CONTROLLER DESIGN

For the control problem of stabilizing the pendulum in the unstable upright equilibrium position while the cart is made to track the desired trajectory, a novel Ant Lion Optimizer tuned

Linear Matrix Inequalities based State Feedback Controller is designed. The output from the optimization problem is the optimal gain of the SFC. Figure 2 depicts the closed loop block diagram used to study the state feedback controllers designed. The performance of Ant Lion Optimizer tuned controller is compared with the LMI based SFC and that of the APSO tuned controller. The design of the control scheme is presented next in detail.

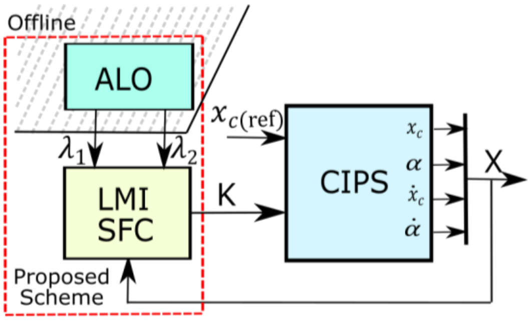

Fig. 2. ALO tuned LMI based SFC.

4.1 Design of LMI based SFC

The linear matrix inequality equations are formed based on the Lyapunov method. The condition for global monotonicity is explained by (Garone and Ntogramatzidis, 2015). For any Linear Time-Invariant system (LTI), there exists a closed-loop feedback gain K such that the system becomes asymptotically stable if there exists $Q = Q^T > 0$ and Z for the inequality problem. $A - BK$ denotes the closed-loop system matrix. If and only if there is a feedback gain K that fulfils Eqn. 14, the closed-loop system stability is ensured.

$$(A - BK)^T P + P(A - BK) < 0 \text{ and } P > 0 \tag{14}$$

A simple change of variables is done so that the feedback gain is also a function of LMI variable. There is a symmetric positive definite matrix Q that has the property of $Q = P^{-1} \text{and } Z = KQ$. The above inequalities are transformed as in Eqn. 15 that defines the inequality problem.

$$(AQ - BZ)^T + (AQ - BZ) < 0, P > 0 \tag{15}$$

The inequality problem in (15) is solved to get the value of Q and Z which is related to the feedback gain by $K = ZQ^{-1}$. The inequality problem is modified to place the poles in the LMI region of the left half of the s-plane which gives an improved transient response. The second inequality equation is thus added to include λ_1 and λ_2 which defines the LMI region on the left half of s-plane where the closed loop poles should lie. The modified inequality problem is shown in Eqn. 17.

$$(AQ - BZ)^T + (AQ - BZ) < 0$$

$$\lambda_1 Q < (AQ - BZ) < \lambda_2 Q \tag{16}$$

The control law is taken to be $u = -Kx$ to minimize the error propagation in the presence of disturbances. The values of λ_1 and λ_2 are to be chosen in such a way that the solution of the inequality problem gives an optimal value of feedback gain K of the SFC. This selection of λ_1 and λ_2 are done by trial and error method. The SFC thus designed should be able to track the desired trajectory while stabilizing the pendulum with minimum tracking error. In the existing LMI based SFC, the optimization / ALO block shown in Figure 2 is not present. The random trial and error λ_1 and λ_2 values are used to solve the inequality problem to get the state feedback gain. For proper selection of λ_1 and λ_2 to give optimal feedback gain 'K', a recent optimization algorithm known as the Ant Lion Optimizer is used to tune the LMI based SFC.

4.2 ALO tuned LMI based SFC

The Ant Lion Optimizer (Mirjalili, 2015) is a nature inspired stochastic (metaheuristic) optimisation algorithm. The algorithm is developed based on the foraging nature of the doodlebugs (Ant Lion). The hunting steps of Ant Lions involve: random walks of ants, building traps, trapping ants in Ant Lion's pits, sliding ants towards Ant Lions, catching ants, and rebuilding the pits.

In the optimisation problem, the ants are similar to the particles in swarm optimisations or an individual in Genetic Algorithms. The ants' position corresponds to that of the values of λ_1 and λ_2 defining the LMI region in inequality Eqn. 16. Each ant is evaluated by using a fitness function during optimization.

The pseudocodes of the algorithm for ALO tuned LMI based SFC is as follows:

Initialise the parameters: Population size, Maximum Iteration, Boundary of search space

Randomly initialise the population of Ants and Ant Lions (λ_1 and λ_2)

Evaluate the fitness of all initial population

Select the fittest Ant Lion as elite

While iteration < max iteration

Determine random walking of ants and select potential ants through roulette wheel

Simulate random walks and select Ant Lions based on their fitness

Check the boundaries to keep the ants within the search space

Calculate the fitness of ants and replace Ant Lion with ants if its fitter

Update elite if Ant Lion becomes fitter than previous elite

Increment iteration and repeat till maximum iteration condition is met

The Integral Square Error (ISE) as given in the Eqn. 17 is taken as the fitness function.

$$fobj = ISE = \sum [y_d(t) - y(t)]^2 \tag{17}$$

In Eqn. 17, $y_d(t)$ is the desired trajectory value and $y(t)$ is the actual output value at t^{th} instant. The block diagram of ALO tuned LMI based SFC is shown in Fig. 2. The ALO algorithm is used for offline tuning of the LMI based SFC. The ALO algorithm finds the elite values of λ_1 and λ_2 which gives the best fitness (minimum Integral Square Error of trajectory tracking) within the search space. The elite values of λ_1 and λ_2 are used in the inequality problem to obtain the optimal state feedback gain which is used in the state feedback controller. For evaluating the performance of the ALO tuned controller, APSO algorithm is also used to tune the LMI based SFC to find the optimum LMI region.

4.3 APSO tuned LMI based SFC

The Adaptive Particle Swarm Optimisation (APSO) is one of the variants of the oldest metaheuristic PSO algorithm developed to avoid local optima saturation. APSO method is an advancement in the existing particle swarm optimization method. The pseudocode for the APSO tuned LMI based SFC is as follows:

Initialize the parameters: Population size, Maximum Iteration, Boundary of search space

Randomly initialize the population of particles (λ_1 and λ_2) position and velocity

While iteration < max iteration

Evaluate the fitness of all initial population ($\sum[y_d(t) - y(t)]^2$)

If fitness is better than fittest update local best and global best

Update inertia weight based on the success rate

Update the velocity and position of particles

Increment iteration and repeat till maximum iteration condition is met

---

The difference in APSO from PSO is that the inertia weight is updated based on the success rate. This enables global exploration and local exploitation. When the success rate is low it indicates that the particles are moving without improvement around the optimum value, whereas a high success rate indicates the particles are converging towards an optimum value. The weights are also adaptively updated based on these success rates. The result of the APSO tuned controller is the optimal gain which is then used in the SFC.

5. RESULTS AND DISCUSSIONS

Detailed comparative study of different SFCs in simulation and experimental investigation of stabilizing the pendulum and tracking the desired trajectory by the cart in the Quanser's IP02 cart-inverted pendulum system is explained in this section.

The rate of convergence and the results obtained depends on several parameters that are initially assigned. The parameters that are chosen initially affect the accuracy of the search results. In both ALO and APSO methods, the population size is taken to be 40 and the number of iterations is taken as 10. For APSO method, few more parameters are initially set. They are $W_{min} = 0.2$, $W_{max} = 0.9$, $V_{max} = 20\%$, $C_1, C_2 = 1.43$. The structure of the ALO algorithm is that it does not get trapped within the local optima and that it is better suited for global exploration. APSO on the other hand has chances for it to be locked in global optima if the velocity and the weights are not updated properly. For similar conditions, the results obtained are shown and discussed next.

The cart-inverted pendulum parameters such as maximum amplitude is set as 20 mm, saturation voltage is set as ±12 V. By trial and error method, the inequality region in LMI based SFC is obtained as $\lambda_1 = -20$ and $\lambda_2 = -3$. This region is taken as the search space for the optimization algorithms. Since the algorithms' results are based on the random initial population, to normalise the data, the optimization problem is repeated 15 times, and the results are recorded for the statistical study of the optimization algorithms' performance. The λ_1, λ_2, closed-loop state feedback gain of the closed-loop system corresponding to the best fitness is shown in Table 2.

Table 2. Results of Optimisation algorithms.

Method	λ_1, λ_2	Feedback Gain (K)
LMI	-20 -3	[-36.9987 65.1271 -26.3948 9.0870]
ALO	-10.008 -3.0017	[-23.5123 46.1916 -18.5787 6.2293]
APSO	-10 -3.0097	[-18.7132 65.3010 -20.6683 9.1041]

The mean, standard deviation, minimum, and maximum of the fitness obtained in both the optimization algorithms are shown in Table 3. From the statistical data, it is clear that the Ant Lion Optimizer has found the best fit solution with the lowest minimum. The mean fitness obtained in the ALO method is also slightly lesser compared to that of the APSO method. The standard deviation of the fitness is slightly higher in the ALO method indicating that the method has wider search space. Even the maximum fitness value of optimization algorithms tuned controllers is less than the LMI based SFC's fitness.

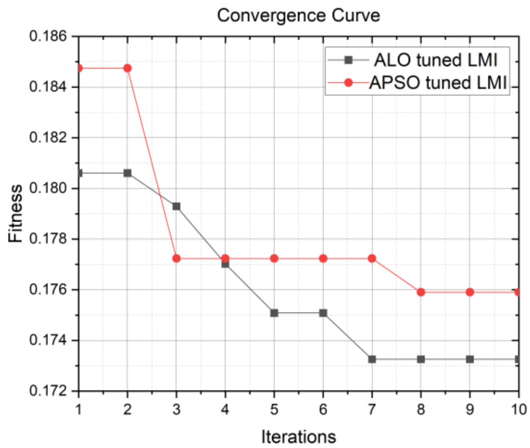

Fig. 3. Convergence Plot.

Table 3. Statistical analysis of Optimisation methods

Method	$fobj_{min}$	$fobj_{mean}$	$fobj_{max}$	$fobj_{\sigma}$
ALO	0.17325	0.183239	0.19291	0.006148
APSO	0.175901	0.183327	0.18762	0.004015
LMI	$fobj$ =0.24680			

The convergence curve of both ALO and APSO methods is shown in Figure 3. The convergence curve implies that the ALO method descends faster towards the optimal value. The final fitness obtained in ALO method is also less compared to that of the APSO method. Figure 4 shows trajectory tracking of the cart for the different SFCs as shown. A square wave of 0.1 Hz, 20 mm peak wave is given as the reference signal. The movement of the cart while stabilizing the pendulum in the upright position is shown. From the plot, it is evident that both the optimization algorithm tuned SFCs can track the desired trajectory. The ALO method has less rise time though the difference is very small. The time-domain values to indicate the performance of trajectory tracking are shown in Table 4.

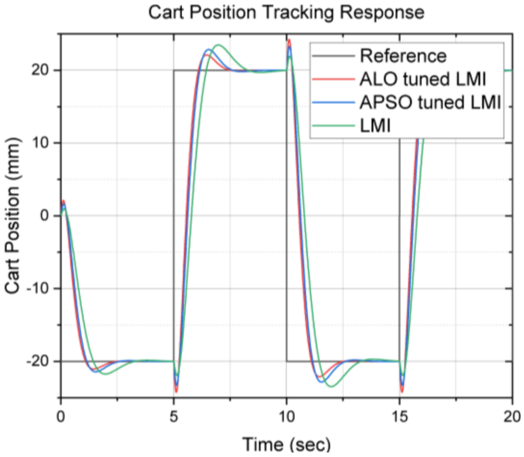

Fig. 4. Cart Position Response.

The rise time, settling time, Peak Overshoot and performance index of the ALO method are slightly lower than that of the APSO method. Thus with minimum initial parameter selection, the ALO method is able to give a slightly better result compared to that of the APSO method.

Table. 4. Comparison of performance during trajectory tracking

Method	Time Domain Values			Performance Index
	Rise Time (t_r) Sec	Settling Time (t_s) Sec	Peak Overshoot (M_p) %	Integral Square Error (ISE)
ALO	0.79	2.52	10.5	0.17325
APSO	0.865	2.62	14.1	0.175901
LMI	1.1	3.29	17.2	0.2468

The pendulum angle variations when the cart is tracking the given reference signal is shown in Figure 5. From the plot, it is clear that the ALO method has minimum pendulum angle variations than that of the APSO method. The dynamic performance of the pendulum angle variations and control input is shown in Table 5. Figure 6 shows the variations of the control input to balance the pendulum and track the desired trajectory. The ALO method has lesser control voltage fluctuations compared to that of the APSO method.

The simulation results from Figures 4 to 6 obtained in MATLAB Simulink indicate that both the SFCs can track the trajectory while the pendulum angle is within the stable operating range of $\pm 5°$. Also, the control input voltage remains within the safe operating range of $\pm 12\,V$ for the motor.

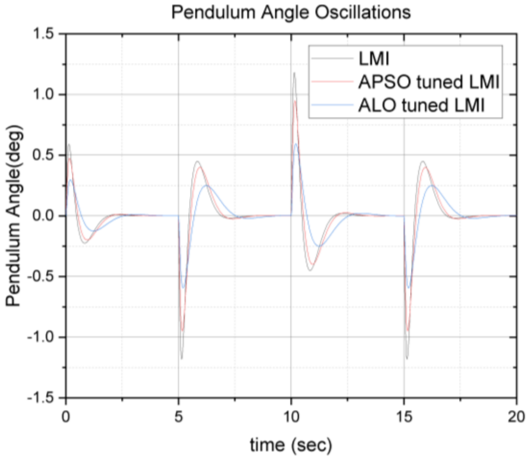

Fig. 5. Pendulum Angle Variations.

Table 5. Maximum Pendulum Angle and Control Input Variations.

Method	Amplitude of Pendulum Angle Oscillations (deg)	Amplitude of Control Input Oscillations (Volts)
ALO	0.5942	0.75
APSO	0.9482	1.704
LMI	1.181	2.676

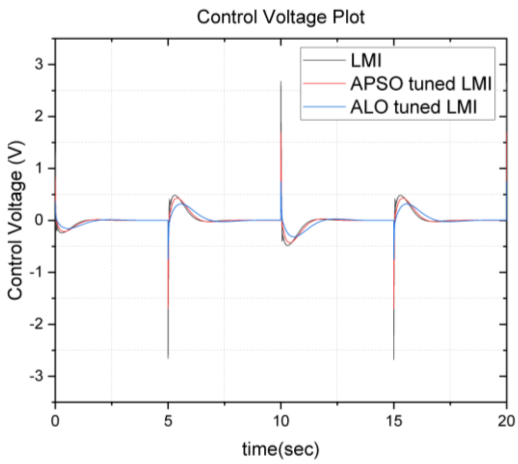

Fig. 6. Control Input Variations.

The rise time and the settling time for the cart position to track the desired square wave trajectory is less in ALO tuned LMI based SFC compared to that of the APSO tuned LMI based SFC. Also, the transient performance including the overshoot is better in ALO tuned LMI based SFC indicating a robust performance. The pendulum angle varies between plus or minus two degrees and the control input variations are also very less which makes the SFCs feasible for experimental investigation.

The block diagram of the real-time experimental setup shown in Figure 7 consists of a PC with MATLAB R2015b, a Quanser's Linear Inverted Pendulum IP02 workstation, a Q2-USB data acquisition board, and a VoltPAQ-X1 Power Amplifier. The ID numbers in Figure 8 indicate the list of all principal elements contained in the IP02 System, as listed in Table 6. In the workstation, the overall rack length is 1.02 m, the overall rack height is 0.061 m and the overall rack depth is 0.15 m.

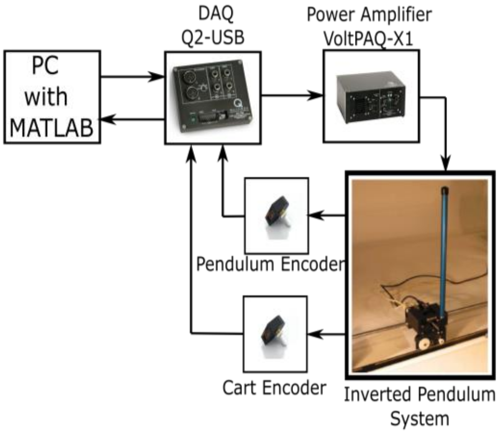

Fig. 7. Experimental Setup for Stabilizing and Trajectory Tracking.

As a safety feature, parts of the rack are kept missing at both ends to prevent the cart from running into the ends and damaging the workstation. The IP02 incorporates a Faulhaber Coreless DC motor (2338S006). This model is a highly efficient low inductance motor that responds significantly faster than a normal DC motor.

Table 6. Components of IP02 system.

ID #	Description	ID #	Description
1	IP02 Cart	10	Cart Encoder Connector
2	Cart Shaft	11	Pendulum Encoder Connector
3	Rack	12	Motor Connector
4	Cart Position Pinion	13	DC Motor
5	Cart Motor Pinion	14	Planetary Gearbox
6	Cart Motor Pinion Shaft	15	Linear Bearing
7	Pendulum Axis	16	Pendulum Socket
8	IP02 Cart Encoder	17	Additional weight
9	IP02 Pendulum Encoder		

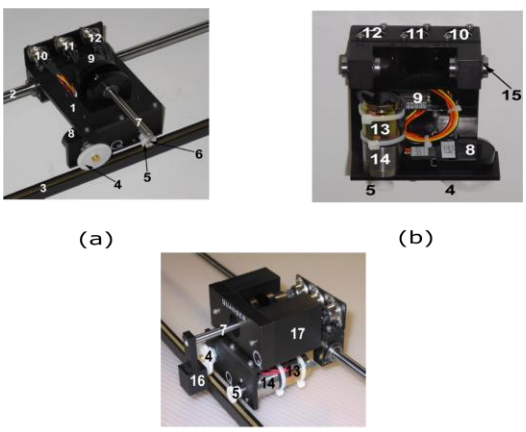

(a) (b) (c)

Fig. 8(a) – IP02 Front View, 8(b) – IP02 Bottom View and 8(c) – Front View of IP02 with weight.

The motor is rated at $\pm 15\,V$, 3 A peak and 1 A during continuous loading conditions. The DC motor is coupled to a Faulhaber Planetary Gearhead Series 23/1 with a gear reduction ratio of 3.71:1. The efficiency of the Gearhead is 88%. To measure cart position and pendulum angle, the workstation has two US Digital S1 single-ended optical shaft encoders with a resolution of 4096 counts per revolution. The cart encoder resolution is 2.275E-005 m/count and the pendulum encoder resolution is 0.0015 rad/count. The number of teeth in the motor pinion is 24 whereas the number of teeth in the position pinion is 56. The power amplifier VoltPAQ-X1 capable of providing $\pm 10\,V$ at 4 A maximum drives the DC motor of the cart in the workstation.

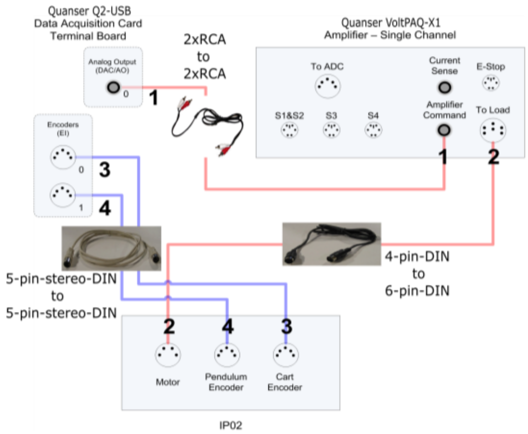

Fig. 9. Hardware Wiring Connection.

The hardware wiring connections are made as shown in Figure 9. The workstation consists of the Quanser's Q2-USB Data acquisition (DAQ) board connected to a PC with MATLAB via the USB port. The Q2-USB DAQ board has provisions for two channels each of Encoder input with quadrature decoding, 12-bit Analog input, and 12-bit Analog output. The Analog Output #0 in the DAQ board is connected to the "Amplifier command" terminal in the power amplifier, to pass the control signal from MATLAB Simulink, using the 2xRCA to 2xRCA connector. The power amplifier supplies the required control voltage to the DC motor from the "To Load" terminal to the "motor connector" terminal in the IP02 cart using the 4-pin-DIN to the 6-pin-DIN connector. The IP02 cart and pendulum shaft angle encoders are connected to Encoder Input #0 and Encoder Input #1 respectively in the DAQ board to pass the cart position and pendulum angle measurements to the SFC in MATLAB using the 5-pin-stereo-DIN to the 5-pin-stereo-DIN connector. During real-time testing, the control scheme implemented in Simulink's external mode with a sampling time of 0.002 s interacts with the workstation through a real-time software called QUARC. The QUARC's *Read Encoder Input* and *Write Analog Output* blocks in Simulink communicate with the hardware through QUARC communications protocols. Based on the error between the desired cart position and the actual cart position, the control signal is passed on to the workstation. This process repeats until the execution is stopped in the Simulink.

The experimental results, for the same operating conditions obtained from the different SFCs in tracking the desired trajectory while maintaining the pendulum in the upright position, are recorded and are shown in Figures 10-12.

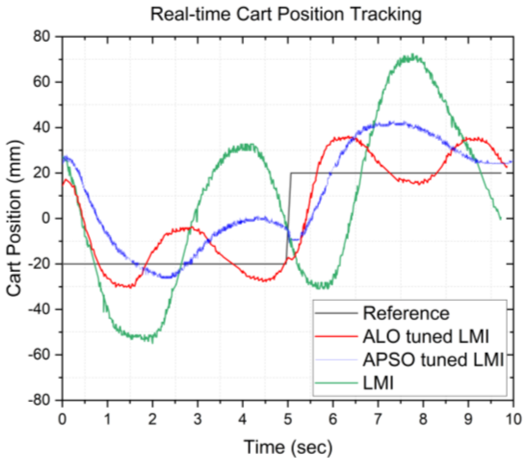

Fig. 10. Real-time Cart Position Response.

From Figure 10, it is observed that the rise time for trajectory tracking by the ALO tuned LMI based controller is less similar to that of the simulation results compared to that of the APSO tuned LMI based SFC and the direct LMI based SFC. The settling time is also slightly less in the case of an ALO-based controller. The cart position oscillates around the desired trajectory for the ALO controller, which shows a faster response to minimize the error and this conforms to the low-performance index (ISE) for the controller as shown in Table 7.

Table 7. Real-time Evaluation Results.

Method	ISE	Maximum Pendulum Angle Oscillations (deg)	Maximum Control Input Oscillations (Volts)
ALO	0.5235	1.1198	1.3870
APSO	0.9022	0.9610	1.4243
LMI	1.9476	1.1281	1.8423

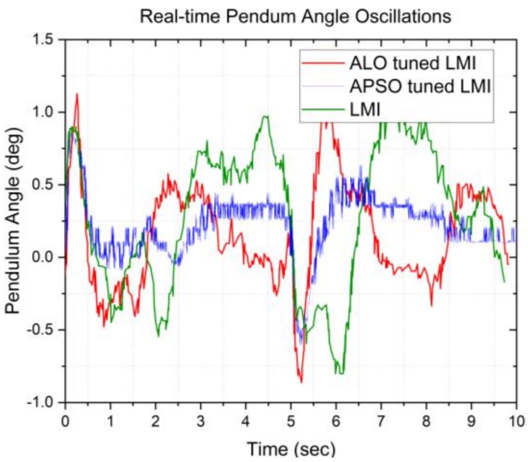

Fig. 11. Real-time Pendulum Angle Variations.

From Figure 11, it is observed that there is not much difference in the pendulum angle oscillations.

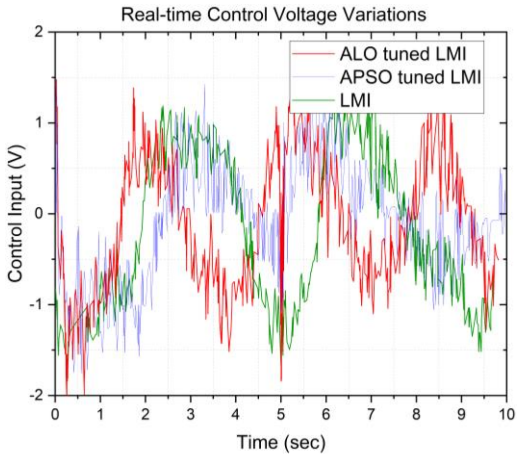

Fig. 12. Real-time Control Input Variations.

The variations of the pendulum angle lie within $\pm 1.25^{\circ}$ for ALO tuned LMI based controller. The control input remains within the safe operating range and the actual value ranges within $\pm 2\,V$ for all the SFCs. Thus, with minimal control effort for one-time offline tuning, ISE of cart position trajectory tracking, and the variation of the pendulum angle is kept within the minimum value by ALO tuned controller compared to that of the APSO tuned controller and LMI based SFC.

6. CONCLUSION

This paper puts forward the Ant Lion Optimizer tuned Linear Matrix Inequality based State Feedback Controller for the improved trajectory tracking of the cart while stabilizing the pendulum in the unstable position. Proper selection of the LMI region is needed to get the optimal performance from the LMI based SFC. The ALO tuned controller is proposed to overcome the cumbersome trial and error method in selecting the LMI region for the Linear Matrix Inequality based State Feedback Controller. Statistical analysis establishes that the precision and search results of the ALO tuned controller is better than the APSO tuned controller and the LMI based SFC without optimization. The Ant Lion Optimizer is preferred over other metaheuristic algorithms because ALO algorithm does not require any parameter initializations like PSO's inertial weight and velocity factor. The proposed controllers' performance is experimentally validated, and the results show that the ALO tuned LMI based SFC has a better transient response while reducing the desired trajectory tracking error by 41.97%, in addition to the stabilization of the inverted pendulum than the APSO tuned controller, which requires proper parameter initialization, and the LMI based SFC without optimisation. Thus, the addition of proposed optimization algorithms in tuning the LMI region improves the performance of the LMI based State Feedback Controller. Further, the suggested ALO tuned controller can be extended to higher-order systems, MIMO systems and for systems with uncertainties as well.

REFERENCES

Abdollahzadeh, B., Gharehchopogh, F. S. and Mirjalili, S. (2021) 'African vultures optimization algorithm: A new nature-inspired metaheuristic algorithm for global optimization problems', Computers and Industrial

Engineering, 158(May), p. 107408. doi: 10.1016/j.cie.2021.107408.

Abualigah, L. et al. (2008) 'Ant Lion Optimizer: A Comprehensive Survey of Its Variants and Applications', IEEE TRANSACTIONS ON SYSTEMS, MAN, AND CYBERNETIC, 39(6), pp. 1362–1382. doi: 10.1007/s11831-020-09420-6.

Adegas, F. D. and Stoustrup, J. (2011) 'Robust structured control design via LMI optimization', IFAC Proceedings Volumes (IFAC-PapersOnline), 44(1 PART 1), pp. 7933–7938. doi: 10.3182/20110828-6-IT-1002.03338.

Alyasseri, Z. A. A. et al. (2018) 'Variants of the flower pollination algorithm: A review', Studies in Computational Intelligence, 744, pp. 91–118. doi: 10.1007/978-3-319-67669-2_5.

Assahubulkahfi, M. et al. (2018) 'LQR tuning by particle swarm optimization of full car suspension system', International Journal of Engineering and Technology(UAE), 7(2.13 Special Issue 13), pp. 328–331. doi: 10.14419/ijet.v7i2.13.13479.

Blondin, M. J. and Pardalos, P. M. (2020) 'A holistic optimization approach for inverted cart-pendulum control tuning', Soft Computing, 24(6), pp. 4343–4359. doi: 10.1007/s00500-019-04198-7.

Boyd, S. et al. (1994) Linear Matrix Inequalities in System and Control Theory, SIAM Studies in Applied Mathematics. doi: 10.1137/1.9781611970777.ch2.

Chang, C. C., Tsai, J. and Pei, S. J. (2012) 'A quantum PSO algorithm for feedback control of semi-autonomous driver assistance systems', 2012 12th International Conference on ITS Telecommunications, ITST 2012, pp. 553–557. doi: 10.1109/ITST.2012.6425240.

Felipe, A. and Oliveira, R. C. L. F. (2021) 'An LMI-Based Algorithm to Compute Robust Stabilizing Feedback Gains Directly as Optimization Variables', IEEE Transactions on Automatic Control, 66(9), pp. 4365–4370.

Franco, E., Astolfi, A. and Rodriguez y Baena, F. (2018) 'Robust balancing control of flexible inverted-pendulum systems', Mechanism and Machine Theory, 130, pp. 539–551. doi: 10.1016/j.mechmachtheory.2018.09.001.

Garone, E. and Ntogramatzidis, L. (2015) 'Linear matrix inequalities for globally monotonic tracking control', Automatica, 61, pp. 173–177. doi: 10.1016/j.automatica.2015.08.009.

Ghaffari, V. (2020) 'A linear matrix inequality–based proportional-derivative sliding mode control tuning method in robotic systems subjected to external disturbance', JVC/Journal of Vibration and Control, 26(23–24), pp. 2297–2315. doi: 10.1177/1077546320921048.

Huang, J. and Ma, Y. (2020) 'Bat algorithm based on an integration strategy and gaussian distribution', Mathematical Problems in Engineering, 2020. doi: 10.1155/2020/9495281.

Irfan, S. et al. (2018) 'Advanced sliding mode control techniques for Inverted Pendulum: Modelling and simulation', Engineering Science and Technology, an International Journal, 21(4), pp. 753–759. doi: 10.1016/j.jestch.2018.06.010.

de Jesús Rubio, J. (2018) 'Discrete time control based in neural networks for pendulums', Applied Soft Computing Journal, 68, pp. 821–832. doi: 10.1016/j.asoc.2017.04.056.

Koch, G. G. et al. (2019) 'Robust H ∞ State Feedback Controllers Based on Linear Matrix Inequalities Applied to Grid-Connected Converters', IEEE Transactions on Industrial Electronics, 66(8), pp. 6021–6031. doi: 10.1109/TIE.2018.2870406.

Kumar E., V. and Jerome, J. (2014) 'An adaptive particle swarm optimization algorithm for robust trajectory tracking of a class of under actuated system', Archives of Electrical Engineering, 63(3), pp. 345–365. doi: 10.2478/aee-2014-0026.

Kwon, O. M. et al. (2006) 'LMI optimization approach to observer-based controller design of uncertain time-delay systems via delayed feedback', Journal of Optimization Theory and Applications, 128(1), pp. 103–117. doi: 10.1007/s10957-005-7560-3.

Li, J., Shang, C. and Zou, M. (2007) 'Parameter Optimization of Linear Quadratic Controller Based on Genetic Algorithm', Tsinghua Science and Technology, 12(SUPPL. 1), pp. 208–211. doi: 10.1016/S1007-0214(07)70111-6.

MacCari, L. A. et al. (2014) 'LMI-based control for grid-connected converters with LCL filters under uncertain parameters', IEEE Transactions on Power Electronics, 29(7), pp. 3776–3785. doi: 10.1109/TPEL.2013.2279015.

Mirjalili, S. (2015) 'The ant lion optimizer', Advances in Engineering Software, 83, pp. 80–98. doi: 10.1016/j.advengsoft.2015.01.010.

Mirjalili, S. et al. (2017) 'Salp Swarm Algorithm: A bio-inspired optimizer for engineering design problems', Advances in Engineering Software, 114, pp. 163–191. doi: 10.1016/j.advengsoft.2017.07.002.

Mirjalili, S. and Lewis, A. (2016) 'The Whale Optimization Algorithm', Advances in Engineering Software, 95, pp. 51–67. doi: 10.1016/j.advengsoft.2016.01.008.

Mirjalili, S., Mirjalili, S. M. and Lewis, A. (2014) 'Grey Wolf Optimizer', Advances in Engineering Software, 69, pp. 46–61. doi: 10.1016/j.advengsoft.2013.12.007.

Muhammad, M. (2018) 'Linear Matrix Inequality-Based State Feedback Control of a Gantry Crane System', Bayero Journal Of Engineering And Technology, 13(2), pp. 106–114.

Ntogramatzidis, L. et al. (2016) 'Globally Monotonic Tracking Control of Multivariable Systems', IEEE Transactions on Automatic Control, 61(9), pp. 2559–2564. doi: 10.1109/TAC.2015.2495582.

da Ponte Caun, R., Assunção, E. and Minhoto Teixeira, M. C. (2021) 'H 2/H ∞ formulation of LQR controls based on LMI for continuous-time uncertain systems', International Journal of Systems Science, 52(3), pp. 612–634. doi: 10.1080/00207721.2020.1836283.

Quanser Inc. (2007), 'SIP User Manual', Canada.

Ravichandran, M. T. and Mahindrakar, A. D. (2011) 'Robust stabilization of a class of underactuated mechanical systems using time scaling and Lyapunov redesign', IEEE Transactions on Industrial Electronics, 58(9), pp. 4299–4313. doi: 10.1109/TIE.2010.2102318.

Roose, A. I., Yahya, S. and Al-Rizzo, H. (2017) ‘Fuzzy-logic control of an inverted pendulum on a cart’, Computers and Electrical Engineering, 61, pp. 31–47. doi: 10.1016/j.compeleceng.2017.05.016.

Rotkowitz, M. and Lall, S. (2006) ‘A Characterization of Convex Problems in Decentralized Control’, IEEE Transactions on Automatic Control, 50(12), pp. 274–286. Available at: http://ieeexplore.ieee.org/xpls/abs_all.jsp?arnumber=1593901.

Saremi, S., Mirjalili, S. and Lewis, A. (2017) ‘Grasshopper Optimisation Algorithm: Theory and application’, Advances in Engineering Software, 105, pp. 30–47. doi: 10.1016/j.advengsoft.2017.01.004.

Scherer, C., Pascal, G. and Mahmoud, C. (1997) ‘Multiobjective Output-Feedback Control via LMI Optimization’, IEEE Transactions on Automatic Control, 42(7), pp. 896–911.

Shahab, E., Nikoobin, A. and Ghoddosian, A. (2017) ‘Indirect-based approach for optimal swing up and stabilization of a single inverted pendulum with experimental validation’, Control Engineering and Applied Informatics, 19(4), pp. 61–71.

Vinodh Kumar, E. and Jerome, J. (2013) ‘Robust LQR controller design for stabilizing and trajectory tracking of inverted pendulum’, in Procedia Engineering. Elsevier Ltd, pp. 169–178. doi: 10.1016/j.proeng.2013.09.088.

Vinodh Kumar, E., Raaja, G. S. and Jerome, J. (2016) ‘Adaptive PSO for optimal LQR tracking control of 2 DoF laboratory helicopter’, Applied Soft Computing Journal, 41, pp. 77–90. doi: 10.1016/j.asoc.2015.12.023.

Werner, H., Korba, P. and Yang, T. C. (2003) ‘Robust tuning of power system stabilizers using LMI-techniques’, IEEE Transactions on Control Systems Technology, 11(1), pp. 147–152. doi: 10.1109/TCST.2002.806449.

Wiboonjaroen, W. and Sujitjorn, S. (2011) ‘Stabilization of an inverted pendulum system via State-PI feedback’, International Journal of Mathematical Models and Methods in Applied Sciences, 5(4), pp. 763–772.

Yang, X. S. and Deb, S. (2014) ‘Cuckoo search: Recent advances and applications’, Neural Computing and Applications, 24(1), pp. 169–174. doi: 10.1007/s00521-013-1367-1.

Yang, X. S. and He, X. (2013) ‘Firefly algorithm: recent advances and applications’, International Journal of Swarm Intelligence, 1(1), p. 36. doi: 10.1504/ijsi.2013.055801.

Zhang, Z. et al. (2019) ‘Antlion optimizer algorithm based on chaos search and its application’, Journal of Systems Engineering and Electronics, 30(2), pp. 352–365. doi: 10.21629/JSEE.2019.02.14.